Néel temperature, the spin fluctuations are frozen out and both the T^2 and the $T^{1/2}$ electron-correlation terms in the resistivity can reflect the true behavior of the electronic effective mass.

We focus in Fig. 3 on the low-temperature behavior of the conductivity for pressures very near the $T = 0$ MI transition. At pressures more than 0.2 kbar above the transition, we observed the usual $T^{1/2}$ form. However, for $P \approx P_c$, the influence of the critical point becomes apparent. A new functional form, $(\sigma - \sigma_0) \sim T^{0.22}$, describes best the dynamical (finite T or ω) response. This unusual exponent follows either from a simple two-parameter least squares fit (0.20 ± 0.07) for $0.035\ K < T < 0.800\ K$ or more precisely (0.22 ± 0.02) from the dynamical scaling analysis discussed below.

Wegner (*18*) proposed a dynamical scaling picture of the $T = 0$ MI transition for noninteracting electrons in a random potential. When these ideas are extended to include interactions in the presence of disorder (*2*, *19*), the electrical conductivity is given by:

$$\sigma(t,T) = b^{-x_\sigma} f(tb^{1/\nu}, Tb^z) \qquad (1a)$$

where x_σ is an unknown exponent, z is the dynamical scaling exponent, ν is the correlation length exponent, f is a scaling function, and b is an arbitrary scale parameter. It follows that:

$$\sigma(t, T = 0) \sim t^{\mu} \text{ and } \sigma(t \to 0, T) \sim T^{x_\sigma/z}, \qquad (1b)$$

with the conductivity exponent $\mu = \nu x_\sigma$. By Eq. 1a, σ/t^μ should be only a function of $T/t^{z\nu}$.

We collapse our conductivity data (*20*) closest to the transition onto such a scaling plot in Fig. 4. The ratio $z\nu/\mu = z/x_\sigma = 4.6 \pm 0.4$ determines the exponent for the first-order correction to σ_0. We then find $\mu = 1.1 \pm 0.2$ by fitting the extracted values of $\mu\ln(t)$ as a function of P, a result in accord with the analysis of the unscaled data of Fig. 1.

Although the data closest to P_c collapse onto a universal scaling curve (Fig. 4), and there is no structural distortion at P_c, we observe a small hysteresis (~1 K) on thermal cycling through the transition (*21*). Presumably, the MI transition is weakly first order, but sufficiently weakly first order to be effectively continuous and to permit the influence of the quantum critical point to emerge. In our efforts to quantify the interplay of statics and dynamics in high-quality single crystals of $NiS_{1.56}Se_{0.44}$, we found that the static critical exponent for the conductivity, $\mu = 1.1 \pm 0.2$, has the value common to most $T \to 0$ continuous MI transitions (*1*), but that the value $x_\sigma/z = 0.22 \pm 0.02$ is unexpected. For noninteracting electrons in three dimensions ($d = 3$), Wegner scaling gives (*18*) $\mu = \nu$ and $x_\sigma/z = 1/3$. Including the effects of electron-electron interactions at the level of a Landau theory for $d > 6$, Kirkpatrick and Belitz (*2*, *22*) find $x_\sigma/z = 2/3$ for $\mu = 1$. By analogy to the random-field Ising model, these authors also point out that hyperscaling should be violated (*22*). An additional experiment would be required to determine if hyperscaling holds for the $Ni(S,Se)_2$ system.

REFERENCES AND NOTES

1. For recent reviews, see P. A. Lee and T. V. Ramakrishnan, *Rev. Mod. Phys.* **57**, 287 (1985), and D. Belitz and T. R. Kirkpatrick, *ibid.* **66**, 261 (1994).
2. T. R. Kirkpatrick and D. Belitz, *Phys. Rev. Lett.* **73**, 862 (1994).
3. S. A. Carter *et al.*, *Phys. Rev. B* **48**, 16841 (1993); T. F. Rosenbaum, in *The Metal-Nonmetal Transition Revisited*, P. P. Edwards and C. N. Rao, Eds. (Taylor and Francis, London, 1995), pp. 105–127.
4. Although $NiS_{2-x}Se_x$ has charge-transfer characteristics, it is commonly analyzed within a Mott-Hubbard framework. See, for example, J. Zaanen, G. A. Sawatzky, J. W. Allen, *Phys. Rev. Lett.* **55**, 418 (1985); A. Y. Matsuura *et al.*, *Phys. Rev. B* **53**, R7584 (1996).
5. H. S. Jarrett *et al.*, *Mater. Res. Bull.* **8**, 877 (1973); F. Gautier *et al.*, *Phys. Lett. A* **53**, 31 (1975); G. Krill and A. Anamou, *J. Phys. Chem. Solids* **41**, 531 (1980); S. Sudo *et al.*, *J. Phys. Soc. Jpn.* **55**, 1806 (1986); X. Yao *et al.*, in *The Metal-Nonmetal Transition Revisited*, P. P. Edwards and C. N. Rao, Eds. (Taylor and Francis, London, 1995), pp. 129–142.
6. For a review, see J. A. Wilson, in *The Metallic and Nonmetallic States of Matter*, P. P. Edwards and C. N. Rao, Eds. (Taylor and Francis, London, 1985), pp. 215–260.
7. R. J. Bouchard, J. L. Gillson, H. S. Jarrett, *Mater. Res. Bull.* **8**, 489 (1973); H. S. Jarrett *et al.*, *ibid.*, p. 877; P. Kwizera, M. S. Dresselhaus, D. Adler, *Phys. Rev. B* **21**, 2328 (1980).
8. X. Yao, T. Hogan, C. Kannewurf, J. M. Honig, preprint.
9. S. Endo, T. Mitsui, T. Miyadai, *Phys. Lett. A* **46**, 29 (1973); T. Miyadai, M. Saitoh, Y. Tazuke, *J. Magn. Magn. Mater.* **104–107**, 1953 (1992).
10. N. Mori *et al.*, *Solid State Physics under Pressure: Recent Advances with Anvil Devices* (Reidel, Dordrecht, 1985), p. 247; J. A. Wilson and G. D. Pitt, *Philos. Mag.* **23**, 1297 (1971).
11. X. Yao and J. M. Honig, *Mater. Res. Bull.* **29**, 709 (1994).
12. K. Kourtakis *et al.*, *J. Solid State Chem.* **76**, 186 (1988).
13. D. D. Klemm, *N. Jahrb. Mineral. Monatsh. J.* **1962**, 32 (1962).
14. T. F. Rosenbaum, S. A. Carter, J. M. Honig, *Rev. Sci. Instrum.* **67**, 617 (1996).
15. W. F. Brinkman and T. M. Rice, *Phys. Rev. Lett.* **27**, 941 (1971); X. Y. Zhang, M. J. Rozenberg, G. Kotliar, *ibid.* **70**, 1666 (1993); Y. Tokura *et al.*, *ibid.*, p. 2126.
16. D. B. McWhan and T. M. Rice, *ibid.* **22**, 887 (1969).
17. B. L. Altshuler, A. G. Aronov, P. A. Lee, *ibid.* **44**, 1288 (1980); T. F. Rosenbaum *et al.*, *ibid.* **46**, 568 (1981).
18. F. J. Wegner, *Z. Phys. B* **25**, 327 (1976).
19. A. M. Finkel'stein, *Sov. Phys. JETP* **57**, 97 (1983); *Sov. Sci. Rev. A* **14**, 1 (1990); C. Castellani, G. Kotliar, P. A. Lee, *Phys. Rev. Lett.* **59**, 323 (1987).
20. The scaling curve is very sensitive to the exact values of t because the temperature dependence of the conductivity is so much smaller than its pressure dependence. Therefore, we allow the product of the normalized pressure and the conductivity exponent, $\mu\ln(t)$, to float, consistent with the uncertainty in our pressure measurement, ±0.03 kbar. By using a log-log scaling plot of σ/t^μ versus $T/t^{z\nu}$, we can determine the best ratio of the exponents $z\nu/\mu$ for the optimal collapse of the data, where no pressure is actually adjusted by more than 0.02 kbar. The kink at $\ln(T/t^{z\nu}) \approx 14$ depends on only one data set and is probably not significant.
21. See also S. Sudo, *J. Magn. Magn. Mater.* **114**, 57 (1992).
22. T. R. Kirkpatrick and D. Belitz, *Phys. Rev. Lett.* **74**, 1178 (1995).

23. We are grateful to D. Belitz for sharing his results prior to publication and to E. Shung for helpful discussions. The work at the University of Chicago was supported by NSF grant DMR95-07873. Y.V.Z. acknowledges support from the NSF REU Program. The work at Purdue University was supported by NSF grant DMR92-22986.

22 July 1996; accepted 22 October 1996

Hf-W Isotopic Evidence for Rapid Accretion and Differentiation in the Early Solar System

Der-Chuen Lee and Alex N. Halliday

The time scales over which inner solar system objects accreted and differentiated are unclear because the isotopic systems of many meteorites are disturbed. ^{182}Hf decays to ^{182}W with a half-life of 9 million years and is a particularly useful chronometer because both elements are highly refractory and immobile. Tungsten isotopic data for IIA, IIIA, IVA, and anomalous iron meteorites and H, L, and LL chondrites indicate that their parent bodies accreted rapidly and segregated metal within just a few million years.

Radionuclides with half-lives on the order of 10^6 to 10^8 years can provide information on the earliest history of the solar system and the nature of the nucleosynthetic events that contributed material to the molecular cloud that collapsed to form the solar nebula (*1–4*). Among various short-lived chronometers, ^{182}Hf-^{182}W [half life, $t_{1/2}$, of 9 million years (m.y.)] is particularly useful for determining the timing of metal-silicate differentiation (such as core formation) in planets and planetesimals (*5–7*). Both Hf and W are highly refractory elements and thus are expected to be in chondritic proportions in much of the solar system, but Hf is strongly lithophile whereas W is moderately siderophile such that the Hf/W ratio in silicate phases will be

Department of Geological Sciences, University of Michigan, Ann Arbor, MI 48109–1063 USA.

much higher than that of coexisting metal. If segregation of metal from silicate occurred within a few half-lives of ^{182}Hf, the isotopic abundance of ^{182}W would eventually be greater in the silicate minerals (with high Hf/W ratios), but would be low in the metal, relative to that found in undifferentiated chondritic material. The magnitude of such an effect in terrestrial W has been used to estimate the age of the Earth's core (6). Here we use the W isotopic compositions of iron meteorites and the metal phases of ordinary chondrites to determine the timing of parent body accretion and the segregation of metallic iron (7)

The W isotopic compositions (8) of various iron and chondritic meteorites and two terrestrial samples are given in Table 1. The new W isotopic composition of each of the carbonaceous chondrites has an uncertainty of $\pm 0.5\ \varepsilon_w$ (9), resulting in a mean of $-0.17 \pm 0.29\ \varepsilon_w$ (Table 1). This value is identical within error to that of the W isotopic composition of the silicate Earth (Fig. 1), providing further support for the suggestion that the Earth's core formed late (6, 7, 10, 11).

A lower limit for the initial ^{182}Hf/^{180}Hf ratio in the solar system of $(2.4 \pm 0.1) \times 10^{-4}$ is provided by the difference between the present day W isotopic composition of carbonaceous chondrites and the least radiogenic W isotopic composition, as measured in the Type IA iron meteorite Arispe (6) Lower estimates based on ion probe studies of zircons in the mesosiderite Vaca Muerta (12) are unreliable, because this meteorite had a multistage evolution and the age of the zircons is uncertain (13, 14). The high initial abundance of ^{182}Hf we deduce has now been predicted from considerations of r-process production of ^{182}Hf in the same supernova source as the actinides, including ^{244}Pu (15).

The model age of a metal (with a low Hf/W ratio) that separated from a chondritic parent can be calculated by comparing its W isotopic composition with that of carbonaceous chondrites (Table 1 and Fig. 1). Similarly, the age differences between metal objects segregated from parents with a chondritic Hf/W ratio can be estimated from the ratio of the differences in W isotopic compositions between each of the metal objects and chondrites. No uncertainties over the Hf/W ratio of chondrites nor the initial Hf isotopic composition of the solar system enter into such model age calculations directly. The time difference between the formation of two metals A and B, Δt_{A-B}, can be expressed as: $\Delta t_{A-B} = [\ln(\Delta W_A/\Delta W_B)]/\lambda$ where ΔW is the difference in ^{182}W/^{184}W ratio between a metal and the mean of the carbonaceous chondrites (Table 1), and λ is the decay constant ($\sim$0.077 m.y.$^{-1}$). This equation can be applied to any parent bodies that had chondritic refractory element ratios regardless of their sizes (16).

We have measured the W isotopic compositions of four iron meteorites (Table 1), including two samples, Cape York (IIIA) and Gibeon (IVA), that have also been studied with ^{107}Pd-^{107}Ag (17). The new W data, combined with the results for Toluca (18), Arispe and Coya Norte (6), cover the range from Type IA through IVA irons plus one anomalous type. All of the samples we analyzed display clear but variable deficits of ^{182}W (Fig. 1) relative to the W isotopic composition in NIST-3163 and carbonaceous chondrites. This result suggests that all the parent bodies of these iron meteorites had differentiated and segregated their metals within the lifetime of ^{182}Hf. Because the Hf/W ratios in iron meteorites are low (19), the W isotopic compositions should have remained unchanged and reflect the W isotopic compositions of the parent bodies at the time of differentiation. Therefore, the apparent model age differences calculated among the iron meteorites should reflect differences in the timing of differentiation of their parent bodies. The resultant model ages span about 7 m.y. (Table 1 and Fig. 1); the greatest age span is for the Type IA samples. The relatively small uncertainty over the decay constant of ^{182}Hf is not included in the error estimates. Most types of iron meteorites display distinct chemical fractionation trends that are thought to result from fractional crystallization within the metallic cores of different planetary bodies. Type IA iron meteorites, however, are thought to be generated by impact melting at the surface of a chondritic parent body (20). Thus, the $\sim$7-m.y. difference between Arispe and Goose Lake may reflect different episodes of impact melting or the melting of surface materials with heterogeneous Hf/W ratios. This range of W model ages falls within the age limit deduced from Pb isotopic compositions of Type I iron meteorites (21). For the other iron meteorites, the model age differences are $\leq$3 m.y. Pd-Ag data (17) indicate an apparent age difference of $\sim 0 \pm 2$ m.y. between Gibeon and Cape York, which is consistent with the Hf-W model age difference of $\sim 2 \pm 3$ m.y. (Table 1 and Fig. 1). Pd-Ag data also indicate an age difference of $\sim 3 \pm 2$ m.y. between the older Tocopilla (IIA) and Gibeon meteorites (17). Coya

Table 1. W isotopic compositions. All the W isotopic measurements are normalized to ^{186}W/^{184}W = 0.927633 (6), except for the sample marked with **. The quoted 2σ standard errors of each measurement refer to the least significant figures. The Hf/W ratios indicate that the effects due to in situ decay of ^{182}Hf would be less than the analytical uncertainties in the W isotopic measurements. The ε_w of each W isotopic measurement is expressed as the deviations relative to the NIST-3163 W standard, which gives a ^{182}W/^{184}W = 0.865000 ± 18 (n = 20), in parts per 10^4. Δt is calculated relative to the age of Arispe. The uncertainty in the W isotopic composition of Arispe is not included in order to show the true time resolution of the ages of different samples. Data marked with * are calculated from (6) and one with ** is from (18).

Sample	^{180}Hf/^{184}W (atomic)	^{182}W/^{184}W	ε_w	Δt (m.y.)
		Terrestrial		
AGV-1		0.865042 ± 31	0.51 ± 0.37	
WS-E		0.864977 ± 48	−0.24 ± 0.56	
		Carbonaceous chondrites (whole rock)		
Allende-1 (USNM 6159)		0.864991 ± 48	−0.10 ± 0.56	
Allende-2 (USNM 6159)		0.864957 ± 45	−0.50 ± 0.50	
Murchison (USNM 5459)		0.864996 ± 45	−0.05 ± 0.50	
Mean		0.864985 ± 25	−0.17 ± 0.29	
		Ordinary chondrites (metal concentrate)		
St. Marguerite (H4)	0.0153	0.864700 ± 41	−3.47 ± 0.47	4 ± 2
Forest Vale (H4)	0.0230	0.864690 ± 50	−3.58 ± 0.58	3 ± 2
Richardton-1 (H5)	0.144	0.864681 ± 44	−3.69 ± 0.51	3 ± 2
Richardton-2 (H5)	0.103	0.864680 ± 31	−3.69 ± 0.36	3 ± 1
Nadiabondi (H5)	0.0661	0.864783 ± 54	−2.51 ± 0.63	8 + 4/−3
Allegan (H5)	0.0517	0.864774 ± 58	−2.61 ± 0.67	8 + 4/−3
Barwell (L5-6)	0.0302	0.864659 ± 47	−3.94 ± 0.54	2 ± 2
Tuxtuac (LL5)	0.00468	0.864805 ± 24	−2.25 ± 0.27	10 ± 2
St. Severin (LL6)	0.0145	0.864718 ± 33	−3.26 ± 0.38	5 ± 2
		Iron meteorites		
Arispe (IA)*		0.864602 ± 77	−4.60 ± 0.89	0
Goose Lake-1 (IA)		0.864753 ± 56	−2.86 ± 0.65	7 + 4/−3
Goose Lake-2 (IA)		0.864764 ± 60	−2.73 ± 0.70	7 + 4/−3
Toluca (IA)**		0.864637 ± 97	−4.20 ± 1.10	1 + 4/−3
Coya Norte (IIA)*		0.864680 ± 90	−3.69 ± 1.20	3 + 5/−3
Cape York (IIIA) (USNM 2145)		0.864689 ± 38	−3.60 ± 0.44	3 ± 2
Gibeon (IVA) (USNM 806)		0.864638 ± 86	−4.18 ± 0.99	1 + 4/−3
Kendall County-1 (An)		0.864696 ± 54	−3.51 ± 0.62	3 + 3/−2
Kendall County-2 (An)		0.864665 ± 70	−3.87 ± 0.70	2 + 4/−3

Norte and Tocopilla are thought to represent fragments of the same meteorite that broke up when entering the Earth's atmosphere or upon impact (in northern Chile). If this is correct, the W isotopic composition of Coya Norte should be identical to that of Tocopilla. Gibeon is ~1 ± 2 m.y. older than Coya Norte, in agreement with the Pd-Ag data (*17*). Our W data are also consistent with a recent study of iron meteorites using the long-lived Re-Os system by Shen *et al.* (*22*). However, these authors reported that IVA irons yielded a Re-Os age of 60 ± 45 m.y. greater than the age of IIA irons (*22*), a substantially larger difference than we found (Fig. 1). Conversely, Smoliar *et al.* (*23*) reported a young apparent Re-Os age for Type IVA irons of 4.464 ± 0.026 billion years ago (Ga). This is more than 70 m.y. younger than the Pb-Pb age of the Allende CAI inclusions (*24*), by which time ^{182}Hf should have become effectively extinct. Yet we see a well resolved W isotopic anomaly of $-4\ \varepsilon_w$ for Gibeon (IVA), indicating that differentiation occurred early, during the lifetime of ^{182}Hf. Type IVA irons appear to have formed within 10 m.y. of Type IIA irons, consistent with ^{107}Pd-^{107}Ag data (*17*). The variations in Re-Os ages most likely reflect the effect of later re-equilibration (*23*).

All the W data from iron meteorites thought to be formed as planetary cores (IIA to IVA and anomalous iron meteorites) are identical within uncertainty. This result indicates that there were only small differences in the timing of core formation in the parent bodies of these meteorites. Placing the Hf-W data into a framework of absolute time would help establish exactly how short the time interval was between accretion and core formation. In this and other respects, a useful comparison can be made with the W isotopic compositions of the metal phases of ordinary chondrites. Unlike carbonaceous chondrites, ordinary chondrites contain reasonably large but variable quantities of segregated metallic iron and exhibit more prominent metamorphic and shock features. They have been assigned to different groups according to their compositions (particularly the iron and siderophile element contents), the ratio of oxidized to metallic iron, and distinct petrologic features (*25*).

We analyzed the W isotopic compositions of metal fractions for eight of the equilibrated chondrites that have been studied previously with the U-Pb system (*26*). Because separation of a pure metal fraction was more difficult for equilibrated chondrites than for iron meteorites, the Hf/W ratios were measured to ensure that they were low. As with iron meteorites, the metals of these ordinary chondrites display resolvable ^{182}W deficits relative to NIST-3163, ranging from ~−3.9 to −2.2 ε_w (Table 1). The data imply that the metal phases in these chondrites separated from the coexisting silicates while ^{182}Hf was still present and that the variations in their W isotopic compositions reflect the relative timing of the fractionation or subsequent re-equilibration. The overall time interval of equilibration for these chondrites is within 10 m.y. after the formation of Arispe (Table 1

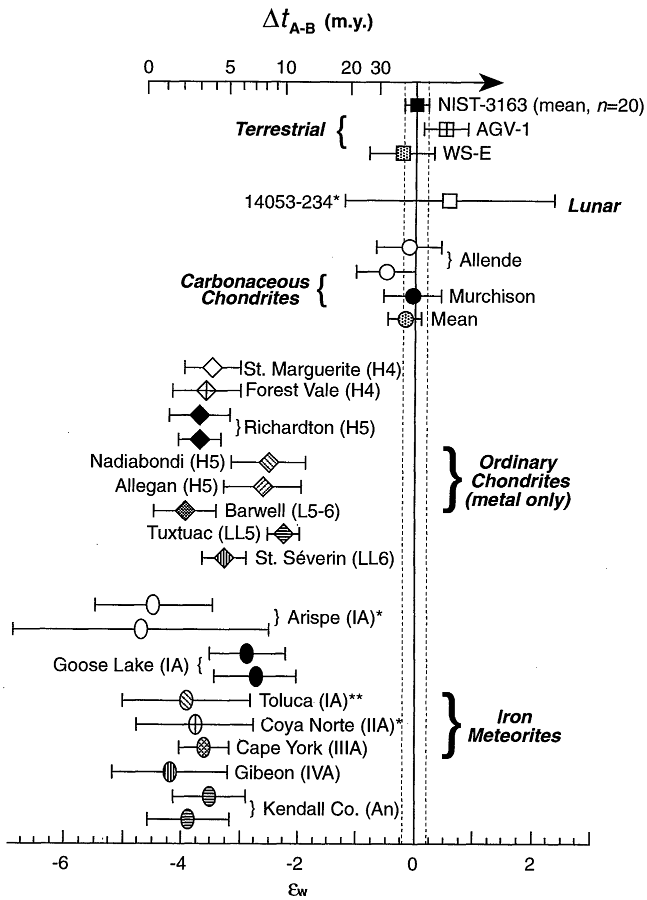

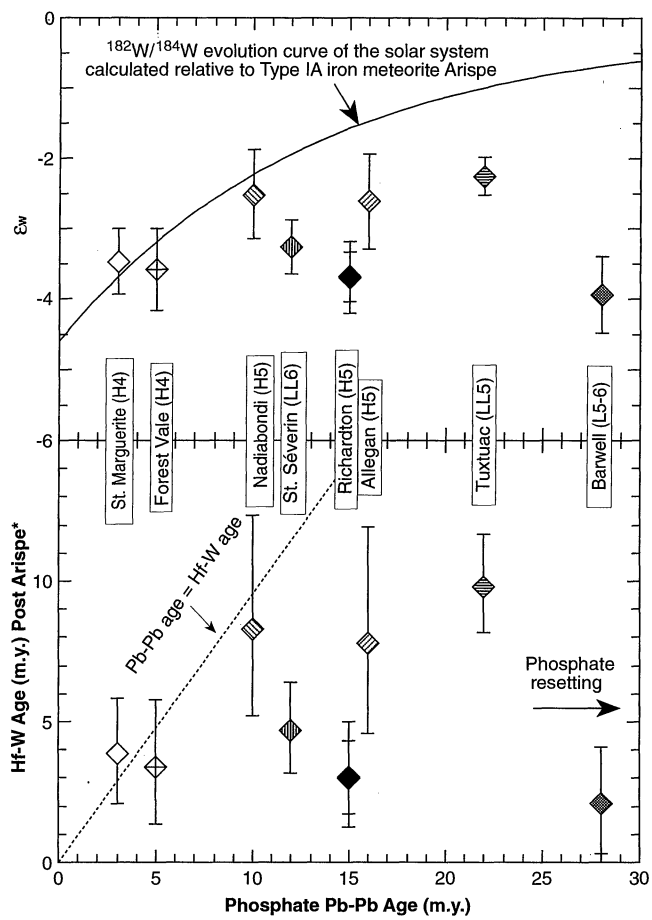

Fig. 1 (left). Δt_{A-B} (m.y.) and ε_w values of samples analyzed in this study (Table 1). Also plotted are renormalized data from (*6*) marked with *, and from (*18*) marked with **. **Fig. 2 (right).** Absolute Pb-Pb ages (m.y.) of phosphates extracted from each of the ordinary chondrites (*26*) versus the measured ε_w and the Hf-W model ages of the metal separates from the same ordinary chondrite (Table 1). The Pb-Pb phosphate ages are expressed as the differences relative to the Pb-Pb age determined for the calcium-aluminum inclusions (CAI) of Allende at 4.566 Ga (*24*). The modeled ^{182}W/^{184}W evolution curve of the solar system with a ^{182}Hf/^{180}Hf initial of 2.4×10^{-4}, deduced from the differences in W isotopic composition between the mean of carbonaceous chondrites (Table 1) and Type IA iron meteorite Arispe (*6*), is shown for reference.

and Fig. 1), which is much smaller than the range of ages deduced from I-Xe data (*27*). Although we have studied only eight ordinary chondrites, discrepancies exist even in samples that have been studied by both methods. For example, I-Xe data indicate that Nadiabondi equilibrated ~16 m.y. earlier than Richardton, whereas W data suggest that Richardton is about 5 ± 3 m.y. older (Fig. 1). The reason why these two extinct nuclide systems are uncorrelated is unclear, although variations in the initial abundance of ^{129}I as a result of incomplete mixing in the solar nebula is a possibility (*27*).

Absolute Pb-Pb ages of the phosphates extracted from these ordinary chondrites (*26*) range from ~3 to 28 m.y. younger than the Pb-Pb age of the Allende CAI inclusions (*24*). Phosphates in equilibrated chondrites are presumably secondary phases produced through oxidation of P-rich metals during thermal processes (*28, 29*). Pb-Pb phosphate ages therefore probably represent the timing of post-equilibration metamorphism within each ordinary chondrite. Allègre *et al.* (*10*) interpreted these data to indicate that the parent body of the H-group of ordinary chondrites formed about 3 m.y. after the Allende CAI inclusions, that is at 4.563 Ga. This result was based on the age of one sample; all the other phosphates, from both the same and other groups yielded younger, though precise, Pb-Pb ages. A comparison between the Pb-Pb phosphate ages and the Hf-W model ages, calculated relative to the Type IA iron meteorite Arispe, shows that the chondrites with the oldest phosphate Pb-Pb ages, St. Marguerite (H4), Forest Vale (H4), and Nadiabondi (H5), have concordant Hf-W model ages consistent with segregation of metals at approximately the same time (Fig. 2). The remaining samples, including two H, one L, and two LL chondrites, exhibit Pb-Pb ages that are significantly younger than the Hf-W model ages (Fig. 2). The excellent agreement between the absolute ages, derived from the long-lived Pb-Pb chronometer, and the Hf-W model ages for the three concordant H chondrites with the oldest Pb-Pb ages, indicates that the initial ^{182}Hf/^{180}Hf for the bulk solar system must be comparable to our estimate of $\geq(2.4 \pm 0.1) \times 10^{-4}$.

Because the Hf-W model ages for the metals most likely reflect the timing of initial equilibration and subsequently remained unchanged, it is understandable that the phosphate Pb-Pb metamorphic ages may be in some cases younger than the time of equilibration (Fig. 2). Göpel *et al.* (*26*) reported a negative correlation between metamorphic grade and Pb-Pb ages among the H type chondrites. Among the three concordant H chondrites, both H4 chondrites appear to be older than the H5 chondrite (Fig. 2), consistent with the inverse correlation suggested by Göpel *et al.* (*26*). Although we studied only five H chondrites, we found no general correlation between Hf-W equilibration age and the metamorphic grade (Fig. 1).

The H, L, and LL chondrites are generally considered to be derived from distinct parent bodies (*30*). The Hf-W model ages indicate that all of these parent bodies formed at about the same time. The striking similarity in W isotopic composition between iron meteorites and the metal phases of ordinary chondrites (Fig. 1) suggests that many iron meteorites simply represent a more extensive style of metal segregation from chondritic parent bodies, all of which probably accreted and differentiated within 10 million years. Such early accretion and planetary differentiation is consistent with ^{53}Mn-^{53}Cr data for some angrites, eucrites, and pallasites (*31–33*), and U-Pb dating of angrites (*34*). The combined data provide a consistent picture of rapid accretion, equilibration, and planetesimal differentiation with small (10^6 year) time differences resolvable between some events. With mounting evidence for rapid accretion and core formation in the inner solar system, there is little doubt that the Earth accreted from such differentiated materials. The question remains as to why the Earth's own metallic core appears to have taken so long to segregate (*6, 7*).

REFERENCES AND NOTES

1. J. H. Reynolds, *Phys. Rev. Lett.* **4**, 8 (1960).
2. T. Lee, D. A. Papanastassiou, G. J. Wasserburg, *Astrophys. J.* **211**, L107 (1977).
3. W. R. Kelly and G. J. Wasserburg, *Geophys. Res. Lett.* **5**, 1079 (1978).
4. J.-L. Birck and C. J. Allègre, *Nature* **331**, 579 (1988).
5. C. L. Harper, J. Völkening, K. G. Heumann, C.-Y. Shih, H. Wiesmann, *Lunar Planet. Sci.* **XX**, 515 (1991).
6. D.-C. Lee and A. N. Halliday, *Nature* **378**, 771 (1995).
7. A. N. Halliday, M. Rehkämper, D.-C. Lee, W. Yi, *Earth Planet. Sci. Lett.* **142**, 75 (1996).

8. All the isotopic measurements were performed with a VG Elemental Plasma 54, which utilizes a multiple collector magnetic sector mass spectrometer equipped with an inductively coupled plasma source. Ions generated by the plasma are accelerated with a high voltage of ~6 kV, applied to both the sample and skimmer cones. The ion beam profile is focused by two sets of d.c. quadrupole lenses and energy-focused by an electrostatic analyzer before entering the magnetic sector. This double-focusing arrangement is capable of producing flat-topped peaks, which are essential for high-precision isotopic measurements. Sample solutions were introduced into the plasma by using the MISTRAL, a highly efficient desolvating nebulizer. The ion source consists of a Fassel-type ICP torch matched with a Henry radio frequency generator, operating at 1.2 to 1.35 kW. The coolant and auxiliary flows were set at roughly 13 and 1 liter per minute, respectively. All the measurements were performed in the static mode and corrected for small isobaric interferences at ^{184}Os and ^{186}Os.
9. All the data are new measurements made on the production MC-ICPMS at the University of Michigan. Terrestrial standard rock AGV-1 and carbonaceous chondrites Allende and Murchison were previously analyzed using a prototype MC-ICPMS instrument (*6*). Tungsten isotopic compositions, isotope dilution ^{180}Hf/^{184}W ratios and duplicates were performed on separate dissolution aliquots (Table 1). $\varepsilon_W = \{[(^{182}W/^{184}W)_{sample}/(^{182}W/^{184}W)_{NIST\text{-}3163}] - 1\} \times 10^4$.

10. C. J. Allègre, G. Manhès, C. Göpel, *Geochim. Cosmochim. Acta* **59**, 1445 (1995).
11. S. J. G. Galer and S. L. Goldstein, in *Earth Processes: Reading the Isotopic Code*, A. Basu and S. R. Hart, Eds. (American Geophysical Union, Washington, DC, 1996), pp. 75–98.
12. T. R. Ireland, *Lunar Planet. Sci.* **XXII**, 609 (1991).
13. ______ and F. Wlotzka, *Earth Planet. Sci. Lett.* **109**, 1 (1992).
14. B. W. Stewart, D. A. Papanastassiou, G. J. Wasserburg, *Geochim. Cosmochim. Acta* **58**, 3487 (1994).
15. G. J. Wasserburg, M. Busso, R. Gallino, *Astrophys. J.* **466**, L109 (1996).

16. Because Hf and W are both highly refractory it is reasonable to assume that most planetesimals that accreted early would have had a chondritic Hf/W ratio. Collisions between large bodies (such as the Earth and a moon-forming impactor) that took place during the late stages of accretion after core formation had already occurred may produce planetesimal-forming debris that might segregate a new core from a parent with high Hf/W ratio (for example, as may have occurred on the moon). Even if the parent body had a chondritic Hf/W ratio, the iron meteorite might represent metal that was segregated at a late stage from a differentiated silicate-rich mantle that had already lost W into its core. Again, the parent reservoir would have a Hf/W ratio greater than the chondritic value. In both situations the deduced Hf-W model age differences would correspond to maximum time differences because the ^{182}W/^{184}W ratio in the reservoir from which the metal was segregated would increase at a faster rate than the ratio in chondritic parent bodies. The main conclusion from our data is that these maximum time differences are short.

17. J. H. Chen and G. J. Wasserburg, in *Earth Processes: Reading the Isotopic Code*, A. Basu and S. R. Hart, Eds. (American Geophysical Union, Washington, DC, 1996), pp. 1–21.
18. C. L. Harper and S. B. Jacobsen, *Geochim. Cosmochim. Acta* **60**, 1131 (1996).
19. J. L. Setser and W. D. Ehmann, *ibid.* **28**, 769 (1964).
20. B.-G. Choi, X. Ouyang, J. T. Wasson, *ibid.* **59**, 593 (1995).
21. C. Göpel, G. Manhès, C. J. Allègre, *ibid.* **49**, 1681 (1985).
22. J. J. Shen, D. A. Papanastassiou, G. J. Wasserburg, *ibid.* **60**, 2887 (1996).
23. M. J. Smoliar, R. J. Walker, J. W. Morgan, *Science* **271**, 1099 (1996).
24. C. Göpel, G. Manhès, C. J. Allègre, 54th Meteoritic Society Meeting Abstract.
25. R. T. Dodd, in *Meteorites: A Petrologic-Chemical Synthesis*, R. T. Dodd, Ed. (Cambridge Univ. Press, New York, 1981).
26. C. Göpel, G. Manhès, C. J. Allègre, *Earth Planet. Sci. Lett.* **121**, 153 (1994).
27. T. D. Swindle and F. A. Podosek, in *Meteorites and the Early Solar System*, J. F. Kerridge and M. S. Matthews, Eds. (Univ. of Arizona Press, Tucson, 1988), pp. 1127–1146.
28. L. H. Ahrens, *Earth Planet. Sci. Lett.* **9**, 345 (1970).
29. C. Perron, M. Bourot-Denise, K. Marti, S. Kim, G. Crozaz, *Meteoritics* **27**, 275 (1988).
30. S. R. Taylor, in *Solar System Evolution a New Perspective*, S. R. Taylor, Ed. (Cambridge Univ. Press, New York, 1992).
31. J.-L. Birck and C. J. Allègre, *Nature* **331**, 579 (1988).
32. G. W. Lugmair, Ch. MacIsaac, A. Shukolyukov, *Lunar Planet. Sci.* **XXV**, 813 (1994).
33. G. W. Lugmair and Ch. MacIsaac, *ibid.* **XXVI**, 879 (1995).
34. G. W. Lugmair and S. J. G. Galer, *Geochim. Cosmochim. Acta* **56**, 1673 (1992).

35. We thank D. Peacor, E. J. Essene, R. Van der Voo, G. J. MacPherson, P. Pellas, and R. Hutchison for permission to access their meteorite collections. We also thank the reviewers for their comments, C. J. Allègre, C. Göpel, and M. W. Johnson for their assistance, and T. R. Ireland, R. J. Walker, and G. J. Wasserburg for discussion. This work was supported by NSF, DOE, NASA, and the University of Michigan.

12 September 1996; accepted 4 November 1996